1 # Lungs contribute to solving the frog's cocktail party problem by

2 # enhancing the spectral contrast of conspecific vocal signals

3

4 <u>Short title:</u> Frogs' lungs help them hear better

5

6 N. Lee[1], J. Christensen-Dalsgaard[2], L. A. White[3,†], K. M. Schrode[4], and M. A. Bee[3,4,*]

7

8 [1] Department of Biology, St. Olaf College, Northfield, MN 55057, USA.

9 [2] Department of Biology, University of Southern Denmark, 5230 Odense M, Denmark.

10 [3] Department of Ecology, Evolution, and Behavior, University of Minnesota - Twin Cities, St.

11 Paul, MN 55108, USA.

12 [4] Graduate Program in Neuroscience, University of Minnesota - Twin Cities, Minneapolis, MN

13 55455, USA.

14

15 <u>Abstract:</u> Noise impairs signal perception and is a major source of selection on animal

16 communication. Identifying adaptations that enable receivers to cope with noise is critical to

17 discovering how animal sensory and communication systems evolve. We integrated biophysical

18 and bioacoustic measurements with physiological modeling to demonstrate that the lungs of

19 frogs serve a heretofore unknown noise-control function in vocal communication. Lung

20 resonance enhances the signal-to-noise ratio for communication by selectively reducing the

21 tympanum's sensitivity at critical frequencies where the tuning of two inner ear organs overlaps.

22 Social network analysis of citizen-science data on frog calling behavior indicates the calls of

23 other frog species in multi-species choruses are a prominent source of environmental noise

24 attenuated by the lungs. These data reveal that an ancient adaptation for detecting sound via the

25 lungs has been evolutionarily co-opted to create spectral contrast enhancement that contributes to

26 solving a multi-species cocktail party problem.

† Current address: National Socio-Environmental Synthesis Center (SESYNC), Annapolis, MD 21401, USA.

* Corresponding author: mbee@umn.edu

INTRODUCTION

Environmental noise is a major source of selection that shapes the evolution of animal sensory and communication systems (*1, 2*). Noise creates problems for effective acoustic communication by increasing signal detection thresholds, disrupting source localization and sound pattern recognition, and impairing auditory discrimination. There is widespread and increasing interest in understanding how animals are adapted to cope with noise problems (*1, 2*), particularly in light of the recent global rise in anthropogenic noise pollution (*3*). For many insects (*4*), frogs (*5*), and birds (*6*) that signal acoustically in large and often multi-species aggregations, the signals of other individuals represent particularly potent sources of environmental noise that reduce the signal-to-noise ratio for communication. In essence, such species must solve multi-species analogs of the human "cocktail party problem," which refers to our difficulty communicating with speech in noisy crowds (*7, 8*). At present, knowledge of the potential diversity of adaptations for solving noise problems among nonhuman animals remains limited.

Frogs represent key taxa for discovering evolved solutions to noise problems (*5, 9, 10*). Among terrestrial vertebrates, acoustic communication evolved independently in frogs some 200 million years ago (*11*), probably soon after the independent evolution during the Triassic of a tympanic middle ear in the lineage leading to modern frogs (*12*). Vocal communication is fundamental to reproduction in most extant frogs. Male frogs aggregate in dense breeding "choruses," often comprising multiple species, where they produce sexual signals termed "advertisement calls" to attract mates and repel rivals (*5, 9, 10*). Advertisement calls are produced at notoriously high sound amplitudes, with peak sound pressure levels (SPL) exceeding 100 dB (at 1 m) in many species (*9*). Consequently, frog choruses are often characterized by high and sustained levels of background noise that may be audible to humans from distances of up to 2 km (*5*). Within the cacophony of a chorus, female frogs must select and locate a mate based on evaluating the advertisement calls of different males (*9*). Chorus noise and the overlapping calls of conspecific and heterospecific males can negatively impact auditory perception and degrade the acoustically-guided mating decisions of females (*5*).

Amphibians are unique among vertebrates in having inner ears with two physically distinct sensory papillae that transduce different frequency ranges of airborne sounds (*9*). In frogs, the two organs are considered "matched filters" in the spectral domain because they are most sensitive to one or more spectral components in conspecific advertisement calls (*9*). The

58   tympanic middle ears of frogs are internally coupled through the mouth cavity via wide and open

59   Eustachian tubes (Fig. 1A) (*13, 14*). Thus, each tympanum's response reflects the summation of

60   sound impinging directly on its external surface and sound reaching its internal surface via input

61   through the opposite, internally coupled tympanum (*13*). In frogs, sound can also reach the

62   internal surface of each tympanum through the body wall and air-filled lungs via the glottis,

63   mouth, and Eustachian tubes (Fig. 1B) (*15-19*). Prior to the evolutionary origins of tympanic

64   middle ears, sound induced vibration of air-filled lungs was a likely mechanism of sound

65   reception in the earliest amphibian ancestors of all tetrapods (*20*). Among extant terrestrial

66   vertebrates, however, the lung-to-ear sound transmission pathway is unique to amphibians.

67   During the respiratory cycle, frog lungs remain continuously pressurized above atmospheric

68   pressure, and they remain inflated for relatively long periods punctuated by brief episodes of

69   ventilation when pulmonary air is expelled through the glottis and then refilled using an active

70   pump mechanism driven by buccal musculature (*18, 21*). Thus, during normal respiration, there

71   is a strong coupling between the lungs and the air-filled tympanic middle ears of frogs. Existing

72   hypotheses for the function of the lung-to-ear pathway include protecting a male frog's hearing

73   during vocalization (*14*) and sharpening the inherent directionality of their internally coupled

74   ears (*15-19*); however, these functions are not yet well understood, and the hypothesis that the

75   lungs improve localization of conspecific signals remains controversial (*13, 22*).

76   Here, we tested a novel hypothesis for the function of the frog's lung-to-ear sound

77   transmission pathway: frog's lungs improve the signal-to-noise ratio for vocal communication by

78   creating *spectral contrast enhancement* (SCE). Spectral contrast refers to the difference in

79   amplitude (in dB) between the "peaks" and "valleys" in a sound spectrum. In the context of

80   human hearing and speech communication, signal processing algorithms for SCE can be used to

81   amplify the formant frequencies (peaks) of voiced speech sounds or attenuate frequencies

82   between adjacent formants (valleys) (*23-25*). SCE can improve speech perception in noise for

83   hearing impaired listeners when implemented as part of the signal processing strategies of

84   hearing aids and cochlear implants (*23-25*). The hypothesis that frogs' lungs function in creating

85   SCE stems from early qualitative reports that tympanic sensitivity can vary as a function of lung

86   inflation (*16-18*). The SCE hypothesis predicts that sound transmission through inflated lungs to

87   the middle ears has one or both of two effects on hearing in frogs. It could selectively augment

88   the ability of sound frequencies emphasized in conspecific advertisement calls to drive vibrations

3

89   of the tympanum. Alternatively, it could selectively reduce the tympanum's sensitivity to non-

90   call frequencies that may be characteristic of sources of environmental noise. We tested these

91   two predictions using the American green treefrog (*Hyla cinerea*; Hylidae), a species in which

92   males call to attract females in noisy breeding choruses, often with multiple other frog species,

93   and females choose their mate based on perceived features of his calls.

94

95   **RESULTS**

96

97   **Inflated lungs selectively reduce tympanum vibrations to non-call frequencies**

98   We used laser vibrometry to assess the impacts of lung inflation on the tympanum's sensitivity

99   across the frequency spectrum and across the horizontal sound field. Using temporarily

100   immobilized females as subjects, we compared the vibration amplitudes of the tympanum in

101   response to free-field acoustic stimulation by broadcasting a frequency modulated (FM) sweep

102   from each of 12 sound incidence angles surrounding the animal (Fig. S1A). Measurements were

103   repeated with the lungs in a naturally inflated state and after manual deflation of the lungs ($n =$

104   21; Fig. 1C). The tympanum was most responsive to frequencies between about 1000 and 5000

105   Hz (Figs. 2A, 2B, S1A). However, in response to frequencies in the range of 1400 to 2200 Hz,

106   tympanum vibration amplitude was substantially reduced, on average by 4 to 6 dB, when the

107   lungs were inflated compared with the deflated state (Fig. 2C). Within this frequency range, the

108   maximum reduction in tympanum vibration amplitude, averaged across individuals (mean ± 95%

109   CI), was 10.0 ± 1.8 dB (range: 3.3 to 17.4 dB) and was significantly nonzero (two-tailed, one-

110   sample t test: $t_{20} = 10.91$, p < 0.001). While the reduction in vibration amplitude spanned the

111   frontal hemifield (Fig. 2C), its bandwidth and magnitude were larger when sound originated

112   from within the contralateral portion of the frontal hemifield (i.e., between 0° and -90°). The

113   modal and median sound incidence angles corresponding to the maximum reduction in

114   tympanum vibration amplitude were -60° and -30°, respectively.

115   We found no evidence that inflated lungs selectively augment the ability of frequencies

116   emphasized in conspecific advertisement calls to drive the tympanum. Similar to other frogs in

117   the genus *Hyla* (*9*), male green treefrogs produce an advertisement call with a frequency

118   spectrum consisting of two prominent spectral peaks that are analogous to the formant

119   frequencies present in human vowel sounds (*26*). The low-frequency peak is important for long-

120   distance communication (*27*) and source localization (*28, 29*), whereas the high-frequency peak

121   appears to be more important in female mate choice (*27, 30*). In a sample of 457 advertisement

122   calls ($\cong$ 20 calls from each of 23 males), the mean ($\pm$ SD) frequencies of the two peaks were 834

123    $\pm$ 14 Hz and 2730 $\pm$ 34 kHz (Fig. 3A). It is worth noting that the mean ($\pm$ SD) frequency of the

124   prominent valley in the frequency spectrum between these two spectral peaks was 1653 $\pm$ 39 Hz,

125   which falls within the range of frequencies (1400 to 2200 Hz) where inflated lungs reduce

126   tympanic sensitivity (Fig. 3A). At the two spectral peaks of conspecific calls, the tympanum's

127   vibration amplitude did not vary as a function of lung inflation. Across angles of sound

128   incidence, the mean ($\pm$ 95 CI) magnitude of the tympanum response at frequencies of 834 Hz

129   and 2730 Hz differed between the inflated and deflated lung states by 0.7 $\pm$ 1.8 dB (Fig. 3B) and

130   0.8 $\pm$ 1.8 dB (Fig. 3C), respectively; these mean values were not significantly different from zero

131   (two-tailed, one-sample t tests: $t_{20} = 0.8$ and $t_{20} = 0.9$, respectively, ps > 0.393). Overall, there

132   was little evidence that inflated lungs augmented the tympanum's response at any specific

133   combinations of frequency and location. Tympanum responses were slightly higher (by 1.3 to 2.7

134   dB on average) at frequencies between 900 and 1500 Hz, but only in a restricted part of the

135   contralateral sound field behind the animal, between about -90° and -180° (Fig. 2C). Other lung-

136   mediated increases in tympanum sensitivity were similarly small and occurred at high

137   frequencies (e.g., between 6000 and 7000 Hz; Fig. 2C) at which both the tympanum and the

138   peripheral auditory nervous system are not very responsive (cf. Figs. 2A, 2B, S1A) (*31, 32*).

139   Together, these data suggest the inflated lungs of frogs function in creating a directionally

140   tuned "notch filter" at the level of the tympana that attenuates a narrow range of sound

141   frequencies predominantly within each contralateral frontal field. Because of this selectivity, the

142   tympanum's sensitivity to the spectral peaks of vocal signals was independent of the state of lung

143   inflation. In fact, the spectrum of the advertisement call has a prominent valley that lacks sound

144   energy at the very frequencies impacted by the lungs.

145

146   **Lung resonance generates a directionally tuned tympanic notch filter**

147   Because the frog's lungs are large air-filled cavities overlain by a relatively thin body wall, they

148   resonate in response to free-field acoustic stimulation (*15, 19*). We hypothesized that the lungs'

149   resonance functions in generating the notch filter that selectively reduces the tympanum's

150   sensitivity. This hypothesis predicts that the peak resonance frequency of the lungs should

151 correspond closely to the frequency range of reduced tympanum sensitivity observed when the

152 lungs are inflated (1400 to 2200 Hz) and that the resonance of the lungs should have a

153 subtractive effect on the tympanum's response within this frequency range.

154 Biophysical measurements revealed that the lungs exhibit a prominent resonance that

155 corresponds closely to the frequency range of the lung-mediated reduction in tympanum

156 sensitivity. We used laser vibrometry to quantify the vibration amplitude of the body wall

157 overlying the lungs in response to free-field acoustic stimulation by an FM sweep broadcast from

158 an ipsilateral position ($n = 10$; Fig S1B). The measured lung resonance had a mean ($\pm$ 95% CI)

159 peak frequency of 1558 ± 89 Hz (range: 1400 Hz to 1850 Hz) and mean ($\pm$ 95% CI) 10-dB down

160 points of 1244 ± 76 Hz and 1906 ± 151 Hz (Fig. 4A). There was a significant negative

161 correlation between peak resonance frequency and body size, as expected if lung volume varies

162 directly with body size (Fig. S2; two-tailed Pearson r = -0.705, $R^2 = 0.498$, p = 0.0228). After

163 manually deflating the lungs, the mean ($\pm$ 95% CI) magnitude of the peak resonance frequency

164 was attenuated by 57.6 ± 6.0 dB and was significantly lower than the magnitude measured in the

165 inflated condition (Fig. 4A; two-tailed, one-sample t test: $t_9 = 18.7$, p < 0.0001). Following

166 manual reinflation of the lungs, the mean ($\pm$ 95% CI) peak frequency of the lung resonance was

167 restored (1627 ± 98 Hz; range: 1450 Hz to 1928 Hz) and did not differ from that measured in the

168 inflated state (Fig. 4A; two-tailed, paired t test: $t_9 = 1.88$, p = 0.0922). These laser measurements,

169 thus, confirmed that under free-field acoustic stimulation, the resonance frequency of inflated

170 lungs corresponds closely to the frequency range of reduced tympanum vibrations when the

171 lungs are inflated.

172 We tested the prediction that inflated lungs have a frequency-specific subtractive effect

173 by comparing reconstructions of the tympanum's free-field response with the lungs inflated

174 versus deflated. To do so, we used local acoustic stimulation (Fig. S1C) to quantify the

175 transmission gain (TG) of indirect sound input to the internal surface of the tympanum via the

176 inflated lungs (TG_L) and the contralateral tympanum (TG_C) (33). Transmission gain represents a

177 relative measure of how efficiently each indirect sound input is coupled to the tympanum. At TG

178 = 0 dB, sounds impinge on the internal and external surfaces of the tympanum with equal

179 amplitudes and interact depending on their relative phases; negative values indicate sound

180 reaches the internal surface of the tympanum at a relatively lower amplitude. The median peak

181 TG_L occurred at 1430 Hz (Fig 4B; $n = 6$ individuals), which falls within the range of the lung's

6

182   peak resonance frequencies measured with free-field acoustic stimulation (1400 Hz to 1850 Hz;

183   cf. Fig. 4A). The peak TG_L was -13 dB (i.e., 13 dB lower) compared with the direct sound input

184   to the tympanum's external surface. The median peak TG_C occurred at 1852 Hz and was -6 dB

185   (i.e., 6 dB lower) compared to direct sound input to the tympanum's external surface (Fig. 4B).

186   Reconstructed tympanic responses to free-field stimulation exhibited the predicted lung-

187   mediated reduction in vibration amplitude in the range of 1400 to 2200 Hz (Fig. 4C). Responses

188   in the deflated state were reconstructed after excluding the lung input from all computations. To

189   reconstruct responses with inflated lungs, we explored a range of transmission gain weightings

190   for TG_L because local stimulation of the body wall (Fig. S1C) underestimates its real magnitude

191   due to the much larger surface area of the body wall exposed to sound during free-field

192   stimulation. At a TG_L weighting of 4×, tympanum responses reconstructed for the inflated lung

193   condition were reduced, relative to the deflated condition, by approximately 4 to 6 dB at -60° in

194   the frequency range of 1400 to 2200 Hz. This reduction is similar in magnitude to that observed

195   in measured free-field responses (Fig. 4C). When this lung-mediated effect was modeled across

196   additional angles of sound incidence, differences in the tympanum's reconstructed free-field

197   responses between the inflated and deflated states revealed broad patterns consistent with those

198   determined with free-field acoustic stimulation: tympanum sensitivity was reduced within the

199   frequency range of 1400 to 2200 Hz when the lungs were inflated, and these reductions were

200   most pronounced at contralateral angles (cf. Figs. 2C and 4D). A transmission gain weighting of

201   4× for TG_L corresponds to a lung transmission gain amplitude that is 12 dB higher than the

202   unweighted value of -13 dB reported above. Our reconstructions, therefore, suggest the peak

203   transmission gain from the lungs is probably closer to -1 dB relative to the direct sound input to

204   the tympanum's external surface and +5 dB relative to the peak transmission gain amplitude

205   from the contralateral tympanum (Fig. 4B). Hence, sound transmission to the internal surface of

206   the tympanum through the lungs is quite substantial and, at the lung resonance frequency, it is

207   nearly equivalent in magnitude to direct sound stimulation of the tympanum's external surface.

208   Together, bioacoustic and biophysical measurements, combined with reconstructing free-

209   field responses, provide direct evidence that the lung resonance generates a directionally tuned

210   "notch filter" that attenuates the contralateral portion of each tympanum's frontal field response

211   within a narrow range of frequencies between 1400 to 2200 Hz. But how might lung mediated

212   notch filtering function in hearing and sound communication? To answer this question, we

7

213   examined the lungs' impacts on tympanic responses in relation both to a physiological model of

214   peripheral frequency tuning in frogs and to the frequency spectra of common sources of

215   environmental noise.

216

217   **Lung mediated notch filtering sharpens peripheral frequency tuning**

218   We modeled peripheral frequency tuning in green treefrogs by estimating frequency tuning

219   curves as 4th order gammatone filters that we parameterized using published data on best

220   excitatory frequencies, bandwidths, and thresholds for 172 auditory nerve fibers in this species

221   (*31*) (Fig. 5). Separate populations of auditory nerve fibers innervating the amphibian papilla are

222   tuned to low frequencies (up to about 700 Hz) and mid-range frequencies (up to about 1300 Hz),

223   whereas a third population of auditory nerve fibers innervating the basilar papilla is more

224   consistently tuned to a common range of higher frequencies (Fig. 5). Consistent with the notion

225   of matched filtering in the spectral domain, the thresholds of auditory nerve fibers innervating

226   the amphibian and basilar papillae are lowest at frequencies matching, respectively, the low-

227   frequency and high-frequency spectral peaks in the advertisement call (Fig. 5).

228   The key finding revealed by this physiological model is that lung-mediated impacts on

229   tympanic sensitivity occur in the frequency range where the tuning of the amphibian and basilar

230   papillae can overlap (Fig. 5). At low amplitudes near threshold, neither inner ear papilla responds

231   to frequencies between 1400 and 2200 Hz. However, the bandwidth of individual auditory nerve

232   fibers broadens considerably at higher sound levels more typical of communication in natural

233   environments, ultimately causing the tuning of the two inner ear papillae to overlap (*32, 34*).

234   Much of the frequency range of overlap between the amphibian and basilar papillae at high

235   sound levels corresponds to the frequency range (1400 to 2200 Hz) where notch filtering by

236   inflated lungs reduces the tympanum's vibration amplitude (Fig. 5). Given this correspondence,

237   the modeled tuning of auditory nerve fibers reveals two possible mechanisms by which the

238   subtractive notch filtering generated by inflated lungs could function to counteract the negative

239   impacts of environmental noise in the frequency range of 1400 to 2200 Hz.

240   First, inflated lungs would reduce energetic masking of conspecific advertisement calls.

241   Consistent with behavioral studies (*34*) and recordings of auditory brainstem responses (*32*),

242   auditory nerve fibers innervating both the mid-frequency region of the amphibian papilla and the

243   basilar papilla are predicted to respond to frequencies in the range of 1400 to 2200 Hz at high

8

244   amplitudes typical of communication. By selectively reducing the sensitivity of the tympanum,

245   notch filtering by inflated lungs would reduce the ability of environmental noise in this

246   frequency range to drive auditory nerve responses that could otherwise mask neural responses to

247   conspecific calls. Second, notch filtering by inflated lungs would reduce two-tone rate

248   suppression along the amphibian papilla. Two-tone rate suppression is a well-known feature of

249   auditory processing in vertebrates (*35*), including green treefrogs (*36, 37*), whereby neural

250   responses to one frequency are suppressed by the addition of a second frequency. In green

251   treefrogs, suppressible auditory nerve fibers with best frequencies between approximately 500

252   and 700 Hz respond to the low-frequency component of conspecific calls at the high amplitudes

253   typical of communication (Fig. 5). Importantly, these fibers are suppressed by simultaneous

254   sound energy between approximately 1400 and 2000 Hz (see Fig. 5 *inset*) (*36, 37*). Thus, notch

255   filtering that selectively attenuates the tympanum's response in this frequency range should

256   additionally reduce two-tone rate suppression of excitatory neural responses to conspecific calls.

257   Our physiological model suggests lung mediated notch filtering functions generally to

258   sharpen peripheral frequency tuning in the range of 1400 to 2200 Hz. This interpretation is

259   consistent with the SCE hypothesis: by selectively attenuating the tympanum's response to

260   frequencies in the valley between the peaks in the conspecific call spectrum, inflated lungs

261   improve the "match" of the peripheral matched filter to frequencies in conspecific signals. This

262   improved match should both reduce energetic masking and two-tone rate suppression that could

263   otherwise impair neural processing of the spectral peaks of conspecific advertisement calls,

264   thereby increasing the neuronal signal-to-noise ratio for communication. A wider band of notch

265   filtering would interfere with tympanic transmission of the spectral peaks in conspecific calls. An

266   important remaining question, therefore, is what sources of environmental noise in the range of

267   1400 to 2200 Hz would be attenuated by lung mediated notch filtering?

268

269   **Lung mediated notch filtering improves the signal-to-noise ratio for communication**

270   For frogs that call in multi-species choruses, the calls of other species breeding at the same times

271   and places represent prominent and behaviorally relevant sources of environmental noise that can

272   interfere with communication (*5, 9*). Therefore, we evaluated the extent to which the calls of

273   syntopically breeding heterospecific frogs constitute environmental noise in the frequency range

274   attenuated by the lungs. To this end, we integrated analyses of continent-scale citizen science

9

275   data from the North American Amphibian Monitoring Program (NAAMP) (*38*) with bioacoustic

276   analyses of archived recordings of frog calls. NAAMP was a long-term (1994-2015) effort to

277   monitor frog populations using roadside calling surveys conducted across 26 states that

278   encompass most of the green treefrog geographic range in the eastern, central, and southern

279   United States. In the NAAMP dataset, there were 19,809 reports of "co-calling" between green

280   treefrogs and a total of 42 other species, meaning these 42 species were observed to call at the

281   same times and places as our focal species (Fig. S3).

282   Social network analysis revealed that just 10 of the 42 co-calling heterospecific species

283   (i.e., 24% of all co-calling species) accounted for the overwhelming majority (79%) of the

284   19,809 observed instances of co-calling between green treefrogs and one or more other species in

285   the NAAMP dataset (Figs. 6 and S3). Of these top-10 heterospecific species, half (i.e., just 5 of

286   42 total heterospecific species) accounted for 42% of all instances of co-calling and produce

287   advertisement calls with prominent spectral peaks falling in the range of 1400 to 2200 Hz (Fig.

288   6). One of these five species, for example, is Fowler's toad (*Anaxyrus fowleri*), which produces a

289   long, loud call with a single spectral peak in the range of 1400 to 2200 Hz (Fig. 6). Others of

290   these five species, such as the barking treefrog (*Hyla gratiosa*), the North American bullfrog

291   (*Lithobates catebeianus*), and the green frog (*Lithobates clamitans*) produce calls with bimodal

292   spectra in which one of two spectral components falls within the range of 1400 to 2200 Hz (Fig.

293   6). We selected these five species' calls for further investigation.

294   To model the impacts of lung mediated notch filtering on the tympanum's response to

295   these five species' calls, we passed the spectra of their advertisement calls through simulated

296   tympanic filters corresponding to 0° (frontal) and -30° and -60° (contralateral) with the lungs

297   inflated versus deflated. We then computed the difference in the tympanum's predicted vibration

298   amplitude between states of lung inflation at the spectral peak of each heterospecific species'

299   calls within or closest to the range of 1400 to 2200 Hz. Consistent with a functional role in noise

300   reduction, the notch filtering generated by inflated lungs reduced the tympanum vibration

301   amplitude in response to the relevant spectral peaks of these five species' calls by approximately

302   4 to 6 dB (Fig. 6; Table S1). The greatest lung-mediated reductions in tympanic responses in the

303   range of 1400 to 2200 Hz occurred for the calls of green frogs (*L. clamitans*), bullfrogs (*L.*

304   *catesbeianus*), and barking treefrogs (*H. gratiosa*) (Fig. 6; Table S1). Notably, bullfrogs and

305   green frogs co-called with green treefrogs most frequently in the NAAMP dataset, with these

10

306   two heterospecific species accounting for 26% of all reported instances of co-calling. Barking

307   treefrogs are the sister species of green treefrogs. The costs of hybrid matings with barking

308   treefrogs have driven evolutionary change in the spectral preferences of female green treefrogs

309   (*39*); therefore, mitigating the risk of mis-mating could be one additional benefit of the lungs'

310   impacts on tympanic responses. Taken together, these data are consistent with the interpretation

311   that SCE created by lung mediated notch filtering improves the signal-to-noise ratio for

312   communication by selectively reducing the tympanum's sensitivity to prominent sources of

313   environmental noise that include the calls of heterospecific frog species in multi-species

314   choruses.

315

316   **DISCUSSION**

317   Resonances of air-filled structures such as lungs or swim bladders improve sound

318   detection in aquatic vertebrates (*40*), and sound detection via the lungs also played important

319   roles in hearing during the evolutionary transition of vertebrates from water to land (*20*). Thus, it

320   is likely that the lungs of the earliest terrestrial vertebrates functioned as accessory sound

321   receiving structures prior to the subsequent evolution of tympanic middle ears (*12*) and acoustic

322   communication (*11*). Our data suggest evolution has co-opted this ancient adaptation for sound

323   reception through the lungs to provide spectral contrast enhancement that improves the signal-to-

324   noise ratio for communication in modern frogs. The inflated lungs of female green treefrogs act

325   as resonators that reduce the tympanum's sensitivity to sounds occurring within a narrow but

326   biologically important range of frequencies. This frequency range, which falls precisely in the

327   valley between the two spectral peaks of the species-specific advertisement call, encompasses

328   frequencies that are transduced by both inner ear papillae and that are used by some of the most

329   frequently encountered heterospecifics in multi-species frog choruses. In essence, inflated lungs

330   enhance spectral contrast by sharpening the peripheral matched filter. In turn, inflated lungs

331   should improve the signal-to-noise ratio for vocal communication by reducing energetic masking

332   and two-tone rate suppression by sources of environmental noise that potentially interfere with

333   processing conspecific calls. Thus, frogs' lungs help them solve a multi-species cocktail party

334   problem.

335   This study's support of the SCE hypothesis suggests the lungs in one major clade of

336   tetrapods serve a heretofore unknown noise-control function in vertebrate hearing and sound

11

337   communication. Moreover, the impact of the frog's inflated lungs on its tympanum vibrations

338   bears striking similarity to SCE in the field of human hearing and speech communication (*23-*

339   *25*). People with sensorineural hearing loss have difficulties understanding speech in noisy social

340   settings that stem, in part, from having broader auditory filters (i.e., reduced frequency

341   selectivity). SCE algorithms can produce a 2 to 4 dB increase in the signal-to-noise ratio that

342   yields significant improvements in word recognition and response times in hearing impaired

343   listeners (*24*). Some SCE algorithms that improve speech recognition for cochlear implant users

344   do so by attenuating the valleys between the peaks of formant frequencies in the speech spectrum

345   without altering the levels of the peaks themselves (*23*). This human engineering solution is

346   functionally similar to how inflated lungs impact tympanic sensitivity in frogs: the state of lung

347   inflation had no impact on the formant-like spectral peaks present in conspecific calls, but

348   inflated lungs attenuated (by up to 10 dB on average) the tympanum's response to frequencies in

349   the valley between them. Notably, lung-mediated notch filtering occurred in the frequency region

350   (1400 to 2200 Hz) where, at high sound levels, the spectral tuning of the separate inner ear

351   organs is broader and frequency selectivity is reduced. In a closely related treefrog, even large

352   changes in lung volume (e.g., 66.7% reduction) yielded no change in the magnitude of the lung's

353   resonance and produced only a small change (e.g., 100 Hz increase) in the peak resonance

354   frequency (*16*). These findings suggest the acoustical properties of the lung input probably

355   change very little over the respiratory cycle. Hence, the lung-to-ear transmission pathway in

356   frogs provides a stable biophysical mechanism for real-time SCE that begins at the tympanum

357   itself. In green treefrogs, such a mechanism should have the effect of enhancing call recognition,

358   though testing this mechanism directly may be impossible due to the difficulty of manipulating

359   lung volume in behaving animals engaged in call recognition tasks. Previous work, however,

360   lends indirect support to the operation of such a mechanism, as call recognition is enhanced

361   when both spectral peaks are present and degraded when additional spectral peaks in the range of

362   1400 to 2200 Hz are artificially added to calls (*26, 37*).

363   A mechanism for SCE might be particularly beneficial to frogs by mitigating negative

364   impacts of the environmental noise created by the calls of other species in a multi-species chorus.

365   Because accurate perception of sexual signals is often tightly linked to evolutionary fitness,

366   species that communicate acoustically in multi-species breeding aggregations can be under

367   intense selection to solve cocktail-party-like problems (*1, 2, 4-7*). The negative impacts of

368   auditory masking caused by background noise and overlapping signals should, thus, favor the

369   evolution of adaptive mechanisms that promote more efficient communication in noise. Results

370   from this study suggest the frog's lung-to-ear sound transmission pathway functions as a novel

371   receiver adaptation to mitigate problems of auditory masking that might be particularly

372   detrimental to effective communication in multi-species choruses.

373   Our results also resolve a longstanding paradox in research on comparative vertebrate

374   hearing. Previous studies of frogs (*13, 16-18*), including green treefrogs (*22*), indicate that the

375   lung-to-ear sound transmission pathway sharpens the tympanum's inherent directional tuning at

376   frequencies corresponding to the lung resonance frequency, but that it has very little (if any)

377   impact on directionality at the signal frequencies used for social and sexual communication with

378   conspecifics. That the frog's lungs improve directional hearing at frequencies not used for

379   communication has remained paradoxical, because increased directionality at conspecific call

380   frequencies would presumably confer selective advantages in the dark and physically complex

381   environment of a nighttime chorus by improving a receiver's ability to locate sources of

382   conspecific calls (e.g., potential mates). A pattern observed but not considered in earlier studies

383   (*16-18*) is that lung-mediated improvements in directionality occur because the tympanum's

384   sensitivity was reduced to sound frequencies near the lung's peak resonance frequency in a

385   direction dependent manner. Our findings resolve the apparent paradox by emphasizing that it is

386   the frequency-dependent, lung-mediated decrease in tympanic sensitivity – and not the

387   associated increase in directionality – that plays a functional role in hearing and sound

388   communication.

389   In conclusion, we propose that natural selection has acted, at least in some frog species,

390   to exploit the lung-to-ear coupling to facilitate perception of conspecific calls in noisy

391   environments by providing a mechanism for real-time spectral contrast enhancement in the

392   auditory periphery. That the frog's lungs play a role in spectral contrast enhancement

393   significantly broadens our understanding of the diversity of evolutionary adaptations to noise

394   problems in nonhuman animals as well as the function of a unique sound transmission pathway

395   in one of the most vocal groups of extant vertebrates.

396

397

MATERIALS AND METHODS

Animals

Subjects were 25 female green treefrogs collected on the grounds of the East Texas Conservation Center in Jasper County, Texas, U.S.A. (30°56'46.15"N, 94°7'51.46"W). Animals were housed in the laboratory on a 12-hour photoperiod, provided with access to perches and refugia, fed a diet of vitamin-dusted crickets, and given ad libitum access to fresh water. All procedures were approved by the Institutional Animal Care and Use Committees of the University of Minnesota (#1401-31258A) and complied with the NIH *Guide for the Care and Use of Laboratory Animals* (8th Edition).

Laser vibrometry measurements

We took laser measurements of 25 frogs (SVL: mean = 54.0 mm, range = 47.7 to 59.2 mm; mass: mean = 12.5 g, range = 8.3 to 17.6 g). For laser measurements, subjects were immobilized with succinylcholine chloride (5 μg/g). Over the 5-10 minutes during which the immobilizing agent took effect, subjects were allowed to regulate their own lung volume. After full immobilization was achieved, lung ventilation had stopped and lung inflation (based on body wall extension) resembled that observed for unmanipulated frogs sitting in a natural posture (*41*). We refer to this state of lung inflation as "inflated." For some procedures, we also examined animals in one or two additional states of lung inflation that involved manually deflating and reinflating the lungs. To create a "deflated" condition, we expressed the air in the animal's lungs by gently depressing the lateral body wall while holding the glottis open with the narrow end of a small, plastic pipette tip. We created a "reinflated" condition by gently blowing air by mouth through a pipette with its tip located just above the closed glottis; the movement of air was sufficient to open the glottis and inflate the lungs. We made every attempt to return the lungs to the natural level of inflation observed prior to manual deflation. When individuals were measured in multiple conditions, we always made measurements in the inflated condition first followed by the deflated condition and then the reinflated condition. While animals were immobilized, we periodically applied water to the dorsum to keep the skin moist to facilitate cutaneous respiration. All laser measurements of an individual subject were made during a single recording session of less than two hours. (Note that temporary manipulations of lung ventilation

14

429 are possible in immobilized frogs because amphibians are capable of cutaneous gas exchange.)

430 We excluded four animals from further analyses (final $n = 21$) because we could not visually

431 confirm their state of lung inflation across treatments.

432   We conducted our experiments in a custom-built, semi-anechoic sound chamber with

433 inside dimensions (L × W × H) of 2.9 m × 2.7 m × 1.9 m (Industrial Acoustics Company, North

434 Aurora, IL). To reduce reverberations inside the chamber, the walls and ceiling were lined with

435 Sonex acoustic foam panels (Model VLW-60; Pinta Acoustic, Inc. Minneapolis, MN). The floor

436 of the chamber was covered in low-pile carpet. During recordings, subjects were positioned on a

437 30-cm tall pedestal made from wire mesh (0.9-mm diameter wire, 10.0-mm grid spacing). The

438 tip of the subject's mandible rested on a raised arch of thin wire, so that the animal sat in a

439 typical posture in the horizontal plane with its jaw parallel to the ground and its head raised and

440 in line with its body. The bottom of the pedestal was suspended 90 cm above the floor of the

441 chamber using a horizontal, 70-cm long piece of Unistrut® attached to its base (Unistrut, Harvey,

442 IL). The Unistrut beam was mounted to a vibration isolation table (Technical Manufacturing

443 Corporation, Peabody, MA) located against an inside wall of the chamber. The Unistrut and

444 vibration isolation table were covered with the same acoustic foam that lined the walls and

445 ceiling of the chamber.

446   We measured the vibration amplitude of the animal's right tympanum or body wall using

447 a laser vibrometer (PDV-100, Polytech, Irvine, CA). The laser was mounted on the same

448 vibration isolation table from which the subject pedestal was mounted. We positioned the laser at

449 approximately 70° to the animal's right relative to the direction in which its snout pointed, which

450 we consider to be 0° (Fig. S1). To enhance reflectance of the laser, a small (45 – 63 μm

451 diameter), retroreflective glass bead (P-RETRO-500, Polytech, Irvine, CA) was placed at the

452 center of the right tympanum and a position on the right, lateral body wall overlying the lung.

453 The analogue output of the laser was acquired (44.1 kHz, 16 bit) using an external digital and

454 analogue data acquisition (DAQ) device (NI USB 6259, National Instruments, Austin, TX) that

455 was controlled by custom software written in MATLAB (v.2014a, MathWorks, Natick, MA) and

456 running on an OptiPlex 745 PC (Dell, Round Rock, TX). The spectra of the acquired laser

457 signals were calculated in MATLAB using the pwelch function (window size = 256, overlap =

458 50%). Laser spectra were corrected for small directional variation in the sound spectrum by

459 subtracting (in dB) the spectrum recorded from a probe microphone from that of the acquired

460   laser signal. In generating heatmaps of tympanum responses (e.g., Fig. 2), we used linear

461   interpolation to determine vibration amplitude values at angles of sound incidence between those

462   measured. Data between measurement points in polar plots were interpolated using a cubic

463   spline.

464

465   **Free-field acoustic stimulation**

466   Acoustic stimuli (44.1 kHz, 16-bit) were broadcast using the same software and hardware used to

467   acquire the laser signal. We controlled signal levels for calibration and playback using a

468   programmable attenuator (PA5, Tucker-Davis Technologies, Alachua, FL). The stimulus

469   consisted of a frequency-modulated (FM) sweep that was 195 ms in duration, had linear onset

470   and offset ramps of 10 ms, and linearly increased in frequency from 0.2 to 7.5 kHz over the 175-

471   ms steady-state portion of its amplitude envelope. Responses were averaged over 20 repetitions

472   of the stimulus. During measurements with the laser, we also recorded acoustic stimuli by

473   positioning the tip of a probe tube of a G.R.A.S. 40SC probe microphone (G.R.A.S. Sound &

474   Vibration A/S, Holte, Denmark) approximately 2 mm from the position on the animal's body

475   (e.g., the right tympanum or its right body wall) from which the laser recorded the response. The

476   microphone's output was amplified using an MP-1 microphone pre-amplifier (Sound Devices,

477   Reedsburg, WI) and recorded using the NIDAQ device.

478   For free-field acoustic stimulation (Fig. S1A, S1B), the stimulus was amplified (Crown

479   XLS1000, Elkhart, IN) and broadcast through a speaker (Mod1, Orb Audio, New York, NY)

480   located 50 cm away from the approximate center of a subject's head (measured along the

481   interaural axis) as it sat on the pedestal. The speaker was attached to a rotating arm covered in

482   acoustic phone and suspended from the ceiling of the sound chamber so that the center of the

483   speaker was at the same height above the chamber floor as the subject and could be placed at any

484   azimuthal position. We presented the stimulus from 12 different angles around the animal (0° to

485   330° in 30° steps; Fig. S1A). An angle of 0° corresponded to the direction in which the animal's

486   snout pointed, +90 corresponded to the animal's right side (ipsilateral to the laser), and -90°

487   corresponded to the animal's left side (contralateral to the laser). For a given subject, we first

488   recorded responses from the tympanum in the inflated condition. We began recordings at a

489   randomly determined location around the subject and then recorded responses at each successive

490   angle after repositioning the speaker in a counterclockwise direction. After making a recording

16

491 from the 12th and final speaker location, we deflated the lungs and remeasured the tympanum

492 beginning at the same randomly determined starting location used in the naturally inflated

493 condition. For a subset of 10 subjects (SVL: mean = 54.4 mm, range = 47.7 to 59.2 mm; mass:

494 mean = 13.1 g, range = 8.3 to 17.6 g), we also measured the vibration amplitude of the body wall

495 overlying the lungs in the inflated and deflated states, as well as after manually reinflating the

496 lungs, with the speaker positioned at +90°. We calibrated the FM sweep to be 85 dB SPL (sound

497 pressure level re 20 µPa, fast, C-weighted) for each speaker position using a Brüel & Kjær Type

498 2250 sound level meter (Brüel & Kjær Sound & Vibration Measurement A/S, Nærum, Denmark)

499 and a Brüel & Kjær Type 4189 ½-inch condenser microphone. For calibration, we suspended the

500 microphone from the ceiling of the sound chamber by an extension cable (AO-0414-D-100) so

501 that it hung at the position a subject's head occupied during recordings.

502

503 **Transmission gain measurements and free-field reconstructions**

504 We used laser vibrometry and local acoustic stimulation of the tympana and body wall to

505 measure the transmission gain of sound input to the tympanum's internal surface via the

506 internally coupled tympanum and the lungs. For local acoustic stimulation (Fig. S1C), we

507 broadcast the same FM sweep used in free-field stimulations through a Sony MDREX15LP

508 earbud (Sony Corporation of America, New York, NY) positioned within approximately 2 mm

509 of either the right tympanum (ipsilateral to the laser), the left tympanum (contralateral to the

510 laser), or the left body wall overlying the left lung (contralateral to the laser) (Fig. S1C). The

511 opening of the earbud was approximately the same diameter as the tympanum. The earbud was

512 positioned using micromanipulators attached to a ring stand placed on the floor of the sound

513 chamber. The tip of a metal probe tube connected to the G.R.A.S. 40SC probe microphone was

514 inserted through the hybrid silicone of the earbud such that its opening barely protruded into the

515 space between the speaker and the acoustically stimulated tympanum or body wall. The output of

516 the probe microphone was amplified with the MP-1 microphone preamplifier and recorded with

517 the NIDAQ data acquisition device. At each location of stimulation, we determined the mean

518 vibration amplitude averaged over response to 20 repetitions of the stimulus with the lungs in the

519 inflated condition.

520   Transmission gains were computed as follows. For each location of stimulation (Fig.

521 S1C), we first computed a transfer function by dividing the average vibration spectrum of the

522   right (ipsilateral) tympanum's response recorded with the laser by the average sound spectrum at

523   each location recorded with the probe microphone. Thus, separate transfer functions were

524   computed for stimulation of the right tympanum (ipsilateral to the laser; $H_I(\omega)$), the left

525   tympanum (contralateral to the laser; $H_C(\omega)$), and the body wall above the lung (contralateral to

526   the laser; $H_L(\omega)$). From these transfer functions, we then computed the transmission gain for

527   sound input to the internal surface of the ipsilateral tympanum via the contralateral tympanum as

528    $TG_C = H_C(\omega) / H_I(\omega)$ and via the lung-to-ear pathway as $TG_L = H_L(\omega) / H_I(\omega)$.

529   Transfer functions measured with local acoustic stimulation allowed us to reconstruct the

530   tympanum's free-field response to sound. To accomplish this, we added the sounds arriving at

531   the tympanum's internal surface via the internally coupled, contralateral tympanum and via the

532   lung-to-ear pathway to the sound measured at the external surface the tympanum. The sound

533   arriving via the contralateral tympanum was computed as the sound impinging on the external

534   surface of the contralateral tympanum (measured with the probe microphone) multiplied by the

535   transmission gain of the contralateral tympanum (TG_C). The sound arriving via the lung-to-ear

536   pathway was computed as the sound impinging on the body wall (measured with the probe

537   microphone) multiplied by the transmission gain of the lung-to-ear pathway as (TG_L). Sound

538   spectra were converted to complex numbers such that all addition was done vectorially and, thus,

539   the resulting sum depended on both the amplitude and phase of each frequency. This sum of

540   sound inputs was then multiplied by the transfer function of the ipsilateral tympanum ($H_I(\omega)$) to

541   arrive at the predicted free-field transfer function. A range of weightings for TG_L (1× to 6×) were

542   explored in reconstructing free-field responses because local acoustic stimulation underestimates

543   the real magnitude of TG_L due to the smaller surface area of the body wall that is stimulated

544   compared with free-field acoustic stimulation.

545

546   **Bioacoustic analyses**

547   We made acoustic recordings of green treefrogs in their natural habitat during active breeding

548   choruses. Between 15 May and 3 July 2013, we recorded 457 advertisement calls from 23 males

549   that were calling in ponds at the East Texas Conservation Center. These recordings (44.1 kHz, 16

550   bit) were made between 2300 and 0200 hours using a Marantz PMD670 recorder (Marantz

551   America, LLC., Mahwah, NJ) and handheld Sennheiser ME66/K6 microphone (Sennheiser

552   USA, Old Lyme CT) held approximately 1 m from the focal animal. Male green treefrogs had a

553   mean (± SD) snout-to-vent length (SVL) of 51.6 ± 3.9 mm and were recorded at a mean air

554   temperature of 20.3 ± 3.0 °C. Recordings of green frogs (*Lithobates clamitans*) (*42*) and

555   bullfrogs (*Lithobates catesbeianus*) (*43*) were obtained during previous studies by one of the

556   authors (MAB); the calls of the remaining eight frog species included in this study were obtained

557   from the Macaulay Library at the Cornell Lab of Ornithology. For each species, we analyzed 6 to

558   23 calls per male (median = 20 calls per male) for each of 9 to 25 males (median = 20 males per

559   species) by computing the power spectrum of each call using MATLAB's pwelch function

560   (window size = 256, overlap = 50%). We determined the average call spectrum for a species by

561   first averaging over the calls recorded from each individual and then over all individuals. Only

562   recordings that were of sufficiently high signal-to-noise ratio and free from excessive

563   background noise were included in these analyses.

564

565   **Model of peripheral frequency selectivity**

566   We modeled frequency selectivity in green treefrogs by creating a bank of hypothetical

567   excitatory frequency tuning curves for 172 auditory nerve fibers. The shape of each modeled

568   tuning curve, plotted as a thin line in Fig. 5, was determined as a 4th order gammatone filter (*44-*

569   *46*). The best sensitivity of each modeled tuning curve was adjusted to match the best excitatory

570   frequency and threshold for a given nerve fiber based on previously published results reported in

571   Fig. 1B of Ehret and Capranica (*31*). The bandwidth of each modeled tuning curve was estimated

572   using the best-fit regression line for Q_{10dB} as a function of threshold [computed based on data

573   from Fig. 2B in Ehret and Capranica (*31*)] to derive a predicted value of Q_{10dB} for each

574   combination of best excitatory frequency and threshold. This estimate was used to compute the

575   corresponding bandwidth 10 dB above threshold for each modeled tuning curve. (The joint

576   relationship between best excitatory frequency, threshold, and bandwidth was not reported

577   directly by Ehret and Capranica for (*31*) individual nerve fibers.)

578

579   **Social network analysis of calling survey data**

580   To generate frog species co-calling networks, we utilized a publicly available dataset from the

581   North American Amphibian Monitoring Program (NAAMP) (*38, 47*). Created as a citizen

582   science collaboration between the United States Geological Survey (USGS) and a collection of

583   state agencies, universities, and non-profit organizations, NAAMP was a long-term effort to

584 monitor frog populations across 26 states in the eastern, central, and southern United States

585 based on roadside calling surveys conducted by trained observers. Details about survey methods

586 can be found elsewhere (*38, 47*). The NAAMP database consists of 319,765 observations of 57

587 identified species made during 21,934 roadside calling surveys conducted between 18 April 1994

588 and 9 August 2015. Fifteen of the 18 states encompassing the geographic range of green

589 treefrogs, which are most abundant in the south-eastern United States, were included in the

590 NAAMP dataset; therefore, coverage was high of geographic areas where green treefrogs were

591 most likely to be heard calling. While the NAAMP dataset does not localize co-calling species

592 precisely to the same body of water or close physical proximity, it represents the best (and only)

593 measure of which other frog species might reasonably be expected to generate environmental

594 noise for a green treefrog receiver in multi-species choruses across its geographic range on a

595 continent-wide scale.

596   To create the co-calling network, we defined a node as a frog species and an edge as an

597 event where both species were reported as calling during the same observation period (typically

598 3 min in duration) on the same date at the same survey stop at the same time. From networks

599 containing only species co-occurring with green tree frogs (Figs. 6, S3), we identified the top ten

600 co-callers by selecting those with the ten highest edge weights. We analyzed networks with and

601 without the inclusion of any species complexes that were not resolved to individual species in the

602 NAAMP dataset (e.g., *Pseudacris feriarum/fouquettei* complex). When using green treefrogs as

603 the focal species, inclusion or exclusion of species complexes did not alter the top ten co-calling

604 species identified. To aid in visualization of the network for Fig. 6, we took the square root of the

605 raw edge weights and scaled this quantity by a factor of 15. All network analyses and images

606 were generated in the *igraph* package in R (Version 3.3.2)(*48*).

607

608 **Statistical analyses**

609 Unless indicated otherwise, a significance criterion of $\alpha = 0.05$ was used. Two-tailed, one-sample

610 t tests were used to test null hypotheses that there were no differences in tympanum vibration

611 amplitude in response to free-field acoustic stimulation between the inflated and deflated states

612 of lung inflation ($n = 21$). A two-tailed Pearson correlation was used to investigate the

613 relationship between the peak frequency of the lungs in the inflated state and snout-to-vent

614 length ($n = 10$). We used a two-tailed, paired-sample t test of the null hypothesis that deflating

20

615   the lungs would not change the magnitude of the peak frequency of the lung's resonance ($n =$

616   10). A two-tailed, paired-sample t test was used to directly compare the magnitudes of the

617   resonance peak of the lungs in the inflated and reinflated states of inflation ($n = 10$). We also

618   used two-tailed, one-sample t tests of the hypothesis that mean magnitudes of reduction in

619   tympanum sensitivity were nonzero for three sound incidence angles (0°, -30°, and -60°) for each

620   of five heterospecific species (15 comparisons total; $n = 21$ individuals for each comparison). All

621   15 comparisons remained significant after using the Holm-Šídák test to control for multiple

622   comparisons; unadjusted P values are reported in Table S1.

623

624   **SUPPLEMENTARY MATERIALS**

625

626   Fig. S1. Laser vibrometry was used to measure the vibration amplitudes of the right tympanum

627   and right body wall overlying the lung in response to acoustic stimulation.

628

629   Fig. S2. Frog lungs are size-dependent resonators.

630

631   Fig. S3. Social network analysis of data from the North American Amphibian Monitoring

632   Program (NAAMP) identified 42 heterospecific, co-calling species.

633

634   Table S1. Lung-mediated reductions in the tympanum's response to frequencies in heterospecific

635   calls.

636

637   **REFERENCES AND NOTES**

638   1.   H. Brumm, Ed., *Animal Communication and Noise*, (Springer, New York, 2013), pp. 453.
639   2.   R. H. Wiley, *Noise Matters: The Evolution of Communication*. (Harvard University
640   Press, Cambridge, MA, 2015), pp. 520.
641   3.   D. M. Dominoni *et al.*, Why conservation biology can benefit from sensory ecology.
642   *Nature Ecology & Evolution* **4**, 502-511 (2020).
643   4.   H. Römer, in *Animal Communication and Noise,* H. Brumm, Ed. (Springer, New York,
644   2013), pp. 33-63.
645   5.   M. A. Bee, Treefrogs as animal models for research on auditory scene analysis and the
646   cocktail party problem. *International Journal of Psychophysiology* **95**, 216-237 (2015).
647   6.   G. M. Klump, in *Psychological Mechanisms in Animal Communication,* M. A. Bee, C. T.
648   Miller, Eds. (Springer, Cham, Switzerland, 2016), chap. 3, pp. 57-88.

649   7.   M. A. Bee, C. Micheyl, The cocktail party problem: What is it? How can it be solved?
650   And why should animal behaviorists study it? *Journal of Comparative Psychology* **122**,
651   235-251 (2008).
652   8.   J. H. McDermott, The cocktail party problem. *Current Biology* **19**, R1024-R1027 (2009).
653   9.   H. C. Gerhardt, F. Huber, *Acoustic communication in insects and anurans: common
654   problems and diverse solutions*. (Chicago University Press, Chicago, 2002), pp. 531.
655   10.   A. S. Feng, J. Schul, in *Hearing and Sound Communication in Amphibians,* P. A. Narins,
656   A. S. Feng, R. R. Fay, A. N. Popper, Eds. (Springer, New York, 2007), pp. 323-350.
657   11.   Z. Chen, J. J. Wiens, The origins of acoustic communication in vertebrates. *Nature
658   Communications* **11**, 1-8 (2020).
659   12.   J. A. Clack, E. Allin, in *Evolution of the Vertebrate Auditory System,* G. A. Manley, A.
660   N. Popper, R. R. Fay, Eds. (Springer, New York, 2004), vol. 22, pp. 128-163.
661   13.   M. A. Bee, J. Christensen-Dalsgaard, Sound source localization and segregation with
662   internally coupled ears: The treefrog model. *Biological Cybernetics* **110**, 271-290 (2016).
663   14.   P. M. Narins, ICE on the road to auditory sensitivity reduction and sound localization in
664   the frog. *Biological Cybernetics* **110**, 263-270 (2016).
665   15.   P. M. Narins, G. Ehret, J. Tautz, Accessory pathway for sound transfer in a neotropical
666   frog. *Proceedings of the National Academy of Sciences of the United States of America*
667   **85**, 1508-1512 (1988).
668   16.   M. B. Jørgensen, Comparative studies of the biophysics of directional hearing in anurans.
669   *Journal of Comparative Physiology A* **169**, 591-598 (1991).
670   17.   M. B. Jørgensen, H. C. Gerhardt, Directional hearing in the gray tree frog *Hyla
671   versicolor:* Eardrum vibrations and phonotaxis. *Journal of Comparative Physiology A*
672   **169**, 177-183 (1991).
673   18.   M. B. Jørgensen, B. Schmitz, J. Christensen-Dalsgaard, Biophysics of directional hearing
674   in the frog *Eleutherodactylus coqui*. *Journal of Comparative Physiology A* **168**, 223-232
675   (1991).
676   19.   G. Ehret, E. Keilwerth, T. Kamada, The lung-eardrum pathway in three treefrog and four
677   dendrobatid frog species: Some properties of sound transmission. *Journal of
678   Experimental Biology* **195**, 329-343 (1994).
679   20.   C. B. Christensen, J. Christensen-Dalsgaard, P. T. Madsen, Hearing of the African
680   lungfish (*Protopterus annectens*) suggests underwater pressure detection and rudimentary
681   aerial hearing in early tetrapods. *The Journal of Experimental Biology* **218**, 381-387
682   (2015).
683   21.   H. De Jongh, C. Gans, On the mechanism of respiration in the bullfrog, *Rana
684   catesbeiana*: A reassessment. *J. Morphol.* **127**, 259-289 (1969).
685   22.   J. Christensen-Dalsgaard, N. Lee, M. A. Bee, Lung-to-ear sound transmission does not
686   improve directional hearing in green treefrogs (*Hyla cinerea*). *bioRxiv*, (2020).
687   23.   W. Nogueira, T. Rode, A. Buchner, Spectral contrast enhancement improves speech
688   intelligibility in noise for cochlear implants. *Journal of the Acoustical Society of America*
689   **139**, 728-739 (2016).
690   24.   T. Baer, B. C. Moore, S. Gatehouse, Spectral contrast enhancement of speech in noise for
691   listeners with sensorineural hearing impairment: Effects on intelligibility, quality, and
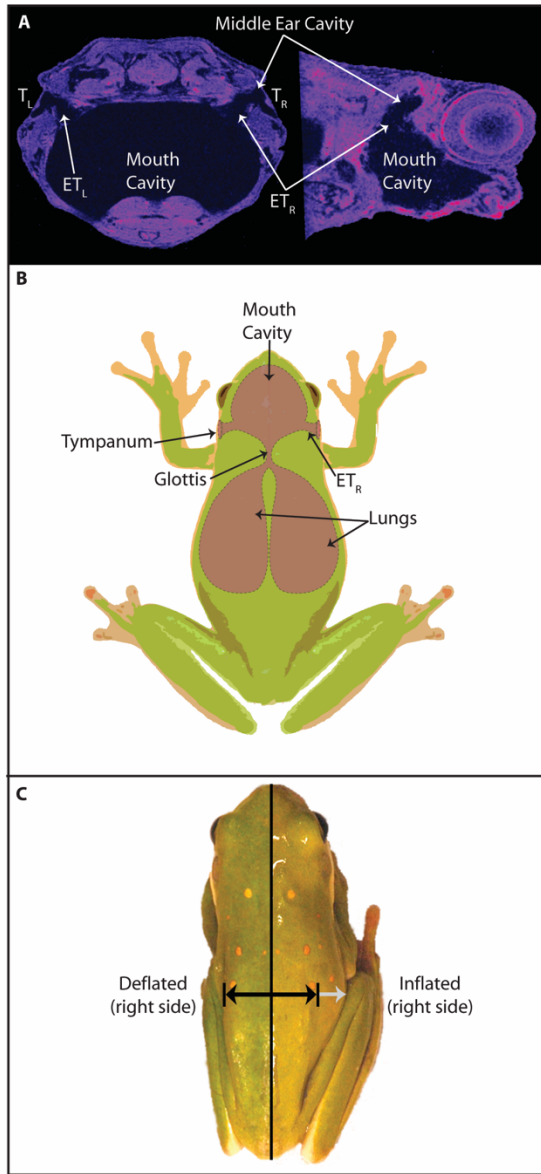692   response times. *Journal of Rehabilitation Research and Development* **30**, 49-72 (1993).

693 25. A. M. Simpson, B. C. J. Moore, B. R. Glasberg, Spectral enhancement to improve the
694   intelligibility of speech in noise for hearing-impaired listeners. *Acta Oto-Laryngol*, 101-
695   107 (1990).
696 26. N. Lee, K. M. Schrode, M. A. Bee, Nonlinear processing of a multicomponent
697   communication signal by combination-sensitive neurons in the anuran inferior colliculus.
698   *Journal of Comparative Physiology A* **203**, 749-772 (2017).
699 27. H. C. Gerhardt, Significance of two frequency bands in long distance vocal
700   communication in the green treefrog. *Nature* **261**, 692-694 (1976).
701 28. J. Rheinlaender, H. C. Gerhardt, D. D. Yager, R. R. Capranica, Accuracy of phonotaxis
702   by the green treefrog (*Hyla cinerea*). *Journal of Comparative Physiology* **133**, 247-255
703   (1979).
704 29. G. M. Klump, J. H. Benedix, H. C. Gerhardt, P. M. Narins, AM representation in green
705   treefrog auditory nerve fibers: Neuroethological implications for pattern recognition and
706   sound localization. *Journal of Comparative Physiology A* **190**, 1011-1021 (2004).
707 30. H. C. Gerhardt, Mating call recognition in the green treefrog (*Hyla cinerea*): Importance
708   of two frequency bands as a function of sound pressure level. *Journal of Comparative
709   Physiology* **144**, 9-16 (1981).
710 31. G. Ehret, R. R. Capranica, Masking patterns and filter characteristics of auditory nerve
711   fibers in the green treefrog (*Hyla cinerea*). *Journal of Comparative Physiology* **141**, 1-12
712   (1980).
713 32. N. P. Buerkle, K. M. Schrode, M. A. Bee, Assessing stimulus and subject influences on
714   auditory evoked potentials and their relation to peripheral physiology in green treefrogs
715   (*Hyla cinerea*). *Comparative Biochemistry and Physiology A* **178**, 68-81 (2014).
716 33. J. Christensen-Dalsgaard, G. A. Manley, Acoustical coupling of lizard eardrums. *Journal
717   of the Association for Research in Otolaryngology* **9**, 407-416 (2008).
718 34. H. C. Gerhardt, Acoustic spectral preferences in two cryptic species of grey treefrogs:
719   Implications for mate choice and sensory mechanisms. *Animal Behaviour* **70**, 39-48
720   (2005).
721 35. M. B. Sachs, E. D. Young, R. H. Lewis, Discharge patterns of single fibers in the pigeon
722   auditory nerve. *Brain Research* **70**, 431-447 (1974).
723 36. G. Ehret, A. J. M. Moffat, R. R. Capranica, Two-tone suppression in auditory nerve
724   fibers of the green treefrog (*Hyla cinerea*). *Journal of the Acoustical Society of America*
725   **73**, 2093-2095 (1983).
726 37. H. C. Gerhardt, G. Höbel, Mid-frequency suppression in the green treefrog (*Hyla
727   cinerea*): mechanisms and implications for the evolution of acoustic communication.
728   *Journal of Comparative Physiology A* **191**, 707-714 (2005).
729 38. T. M. Foreman, E. H. C. Grant, L. A. Weir, in *U.S. Geological Survey data release*.
730   (2017).
731 39. G. Höbel, H. C. Gerhardt, Reproductive character displacement in the acoustic
732   communication system of green tree frogs (*Hyla cinerea*). *Evolution* **57**, 894-904 (2003).
733 40. A. N. Popper, R. R. Fay, Rethinking sound detection by fishes. *Hearing research* **273**,
734   25-36 (2011).
735 41. M. S. Caldwell *et al.*, Spatial hearing in Cope's gray treefrog: II. Frequency-dependent
736   directionality in the amplitude and phase of tympanum vibrations. *Journal of
737   Comparative Physiology A* **200**, 285-304 (2014).

738 42. M. Bee, C. Kozich, K. Blackwell, H. Gerhardt, Individual variation in advertisement calls
739   of territorial male green frogs, Rana clamitans: Implications for individual discrimination.
740   *Ethology* **107**, 65-84 (2001).
741 43. M. Bee, H. Gerhardt, Neighbour-stranger discrimination by territorial male bullfrogs
742   (Rana catesbeiana): I. Acoustic basis. *Animal Behaviour* **62**, 1129-1140 (2001).
743 44. N. Lee, J. L. Ward, A. Vélez, C. Micheyl, M. A. Bee, Frogs exploit statistical regularities
744   in noisy acoustic scenes to solve cocktail-party-like problems. *Current Biology* **27**, 743-
745   750 (2017).
746 45. R. D. Patterson, I. Nimmo-Smith, J. Holdsworth, P. Rice, in *A Meeting of the IOC Speech
747   Group on Auditory Modelling at RSRE*. (1987), vol. 2.
748 46. V. Hohmann, Frequency analysis and synthesis using a Gammatone filterbank. *Acta
749   Acustica united with Acustica* **88**, 433-442 (2002).
750 47. L. A. Weir, M. J. Mossman, in *Amphibian Declines: Conservation Status of United States
751   Species,* M. J. Lannoo, Ed. (University of California Press, Berkeley, 2005), pp. 307-313.
752 48. G. Csardi, T. Nepusz, The igraph software package for complex network research.
753   *InterJournal, Complex Systems* **1695**, 1-9 (2006).
754 49. H. C. Gerhardt, Sound pressure levels and radiation patterns of vocalizations of some
755   North American frogs and toads. *Journal of Comparative Physiology* **102**, 1-12 (1975).
756 50. J. C. Tanner, M. A. Bee, Within-individual variation in sexual displays: signal or noise?
757   *Behavioral Ecology* **30**, 80-91 (2019).
758

Figure 1

Fig. 1. Sound transmitted via the lungs reaches the internal surfaces of the frog's internally coupled tympana. (A) Magnetic resonance images (coronal, left; sagittal, right) of a green treefrog head showing the internal coupling of the left (L) and right (R) tympana (T) and air-filled middle ear cavities through the Eustachian tubes (ET) and mouth cavity. **(B)** Schematic illustration showing the coupling of the lungs through the glottis to the internally coupled tympana. **(C)** A split image of a female green treefrog showing the lateral extension of her right body wall in the inflated (non-reflected right half of image) and deflated (reflected left half of image) states of lung inflation. Black arrows depict the lateral extension of the female's right body wall in the deflated state, and the light gray arrow depicts the additional lateral extension of the right body wall in the inflated condition.

Figure 2
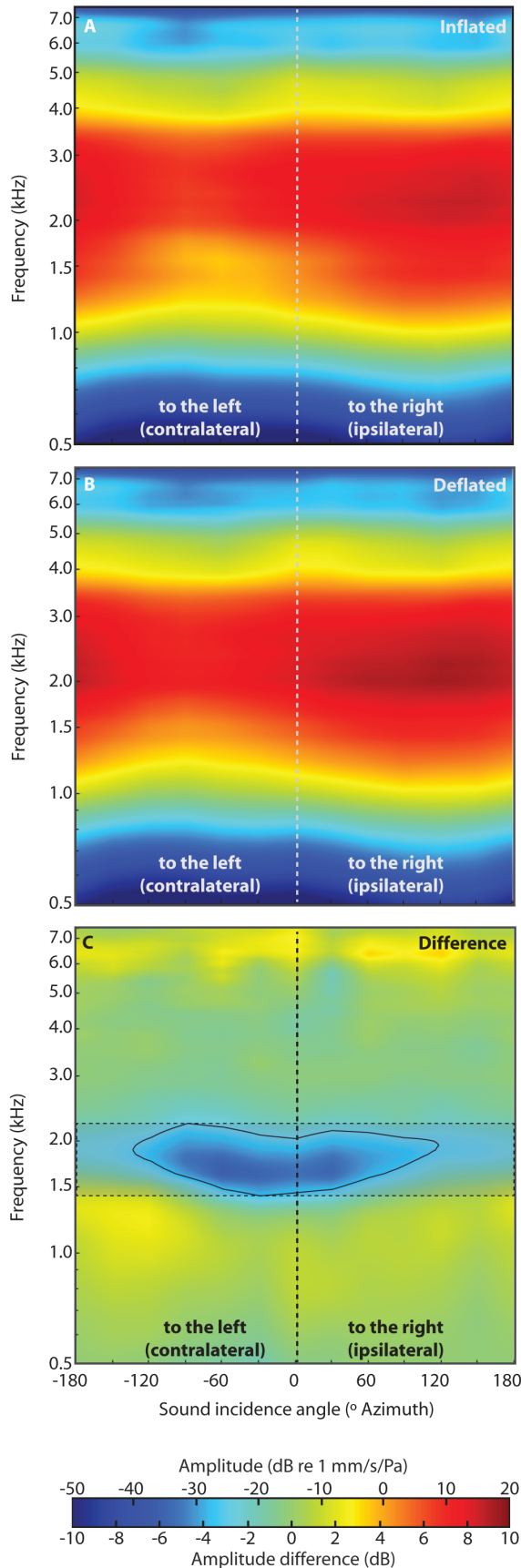
Fig. 2. Inflated lungs selectively reduce tympanum vibrations in the frequency range of 1400 to 2200 Hz. (A-B) Heatmaps showing the mean vibration amplitudes of the right tympanum measured using laser vibrometry in response to free-field acoustic stimulation by an FM sweep presented from each of 12 sound incidence angles (0° to ±180° in 30° steps) surrounding the animal (Fig. S1A). Measurements were repeated in the inflated **(A)** and deflated **(B)** states of lung inflation ($n = 21$ individuals). **(C)** Heatmap showing the mean differences between the vibration amplitudes of the tympanum in the inflated and deflated states of lung inflation (inflated – deflated) across frequency and sound incidence angle ($n = 21$ individuals). The black contour encloses frequencies and angles where inflated lungs reduced vibration amplitudes by ≥ 4 dB. The minimum and maximum frequencies enclosed by the contour are 1400 Hz and 2200 Hz, respectively. The dashed lines and shaded box enclose frequencies between 1400 Hz and 2200 Hz across all angles and are reproduced in subsequent figures.

26

Figure 3
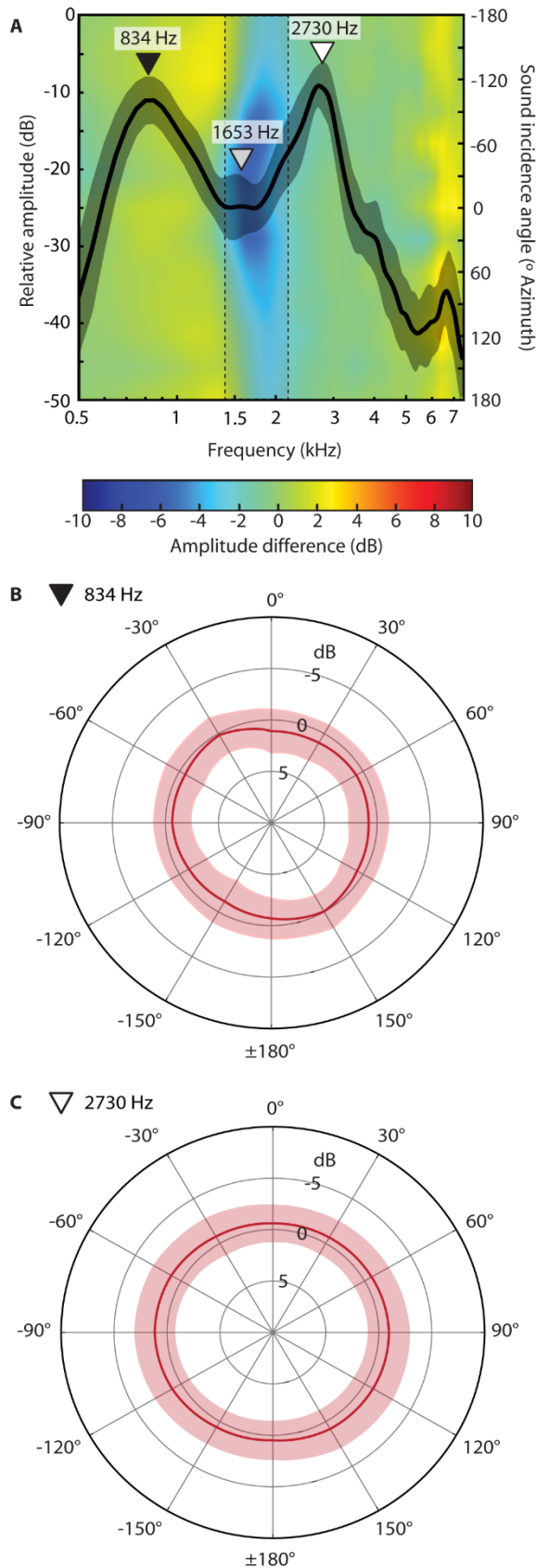
Fig. 3. Inflated lungs selectively reduce tympanum vibrations to non-call frequencies. (A) Frequency spectrum of the green treefrog advertisement call overlaid on a heatmap showing lung-mediated effects on tympanic sensitivity (redrawn from Fig. 2C and rotated 90° clockwise). The spectrum consists of two prominent spectral components, a low-frequency peak (834 Hz, black triangle) and a high-frequency peak (2730 Hz, white triangle) separated by a prominent valley in the spectrum centered at 1653 Hz (gray triangle). The thick black line and shaded gray area depict the mean ± 1 SD call spectrum (n = 23 males, 457 individual calls). The dashed lines and shaded box enclose frequencies between 1400 Hz and 2200 Hz across all angles. (B, C) Polar plots showing the mean ± 95% CI difference (in dB) in the tympanum's response between the inflated and deflated conditions (inflated – deflated) at the frequencies of the two spectral components of conspecific calls. The 95% CIs included 0 dB at all angles of sound incidence.

Figure 4
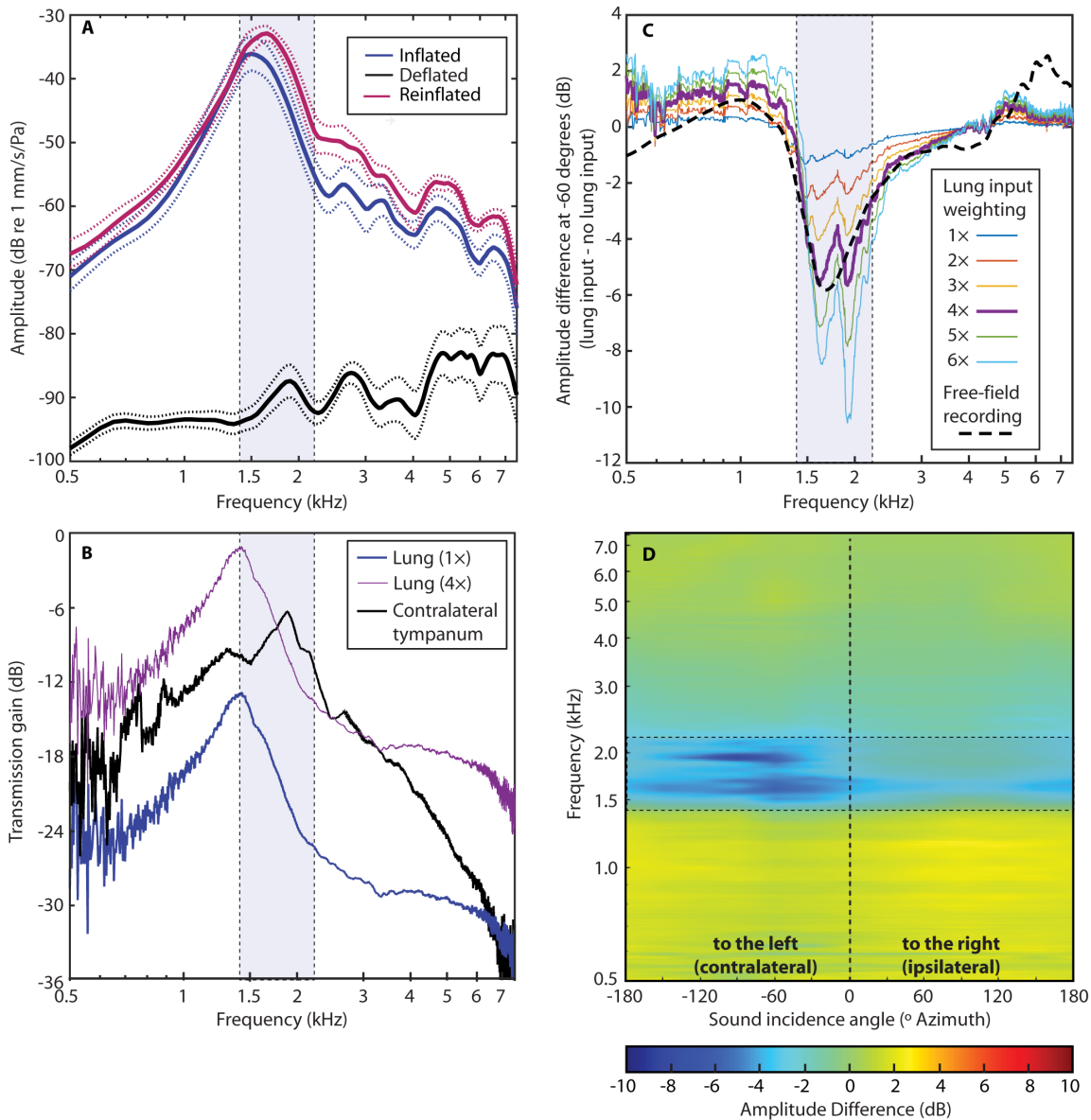
Fig. 4. Lung resonance generates a tympanic notch filter. (A) Under free-field acoustic stimulation by an FM sweep, the inflated lungs of green treefrogs resonate at frequencies between 1200 to 1900 Hz. Depicted here are the mean (solid lines; $n = 10$ individuals) ± 95% CIs (dashed curves) vibration amplitudes of the body wall above the right lung in the inflated, deflated, and reinflated conditions. **(B)** Transmission gain of indirect sound input to the internal surface of the ipsilateral tympanum from the lungs (TG$_L$, with 1× and 4× transmission gain weightings) and contralateral tympanum (TG$_C$) measured under conditions of local acoustic stimulation by an FM sweep (Fig. S1C). **(C)** Predicted effects of inflated lungs based on reconstructing the tympanum's free-field response at a contralateral sound incidence angle of -60° using measures of transfer functions obtained under conditions of local acoustic stimulation by an FM sweep. Differences between reconstructed tympanum responses for the inflated and deflated conditions are shown for six transmission gain weightings (1× to 6×) of the lung input to

account for the fact that the lungs would be stimulated to a much larger degree under free-field acoustic conditions. The actual impacts of the lung on the tympanum's free-field response are shown by the dashed black line (redrawn from the -60° contour in the heatmap in Fig. 2C), which closely matches the predicted response for a lung transmission gain weighting of 4×. **(D)** Predicted effects of inflated lungs on the tympanum's free-field response at all angles of sound incidence based on measures of transfer functions under conditions of local acoustic stimulation by an FM sweep and using a lung input weighting of 4×. In all panels **(A-D)**, the dashed lines and shaded blue rectangle enclose frequencies between 1400 Hz and 2200 Hz.
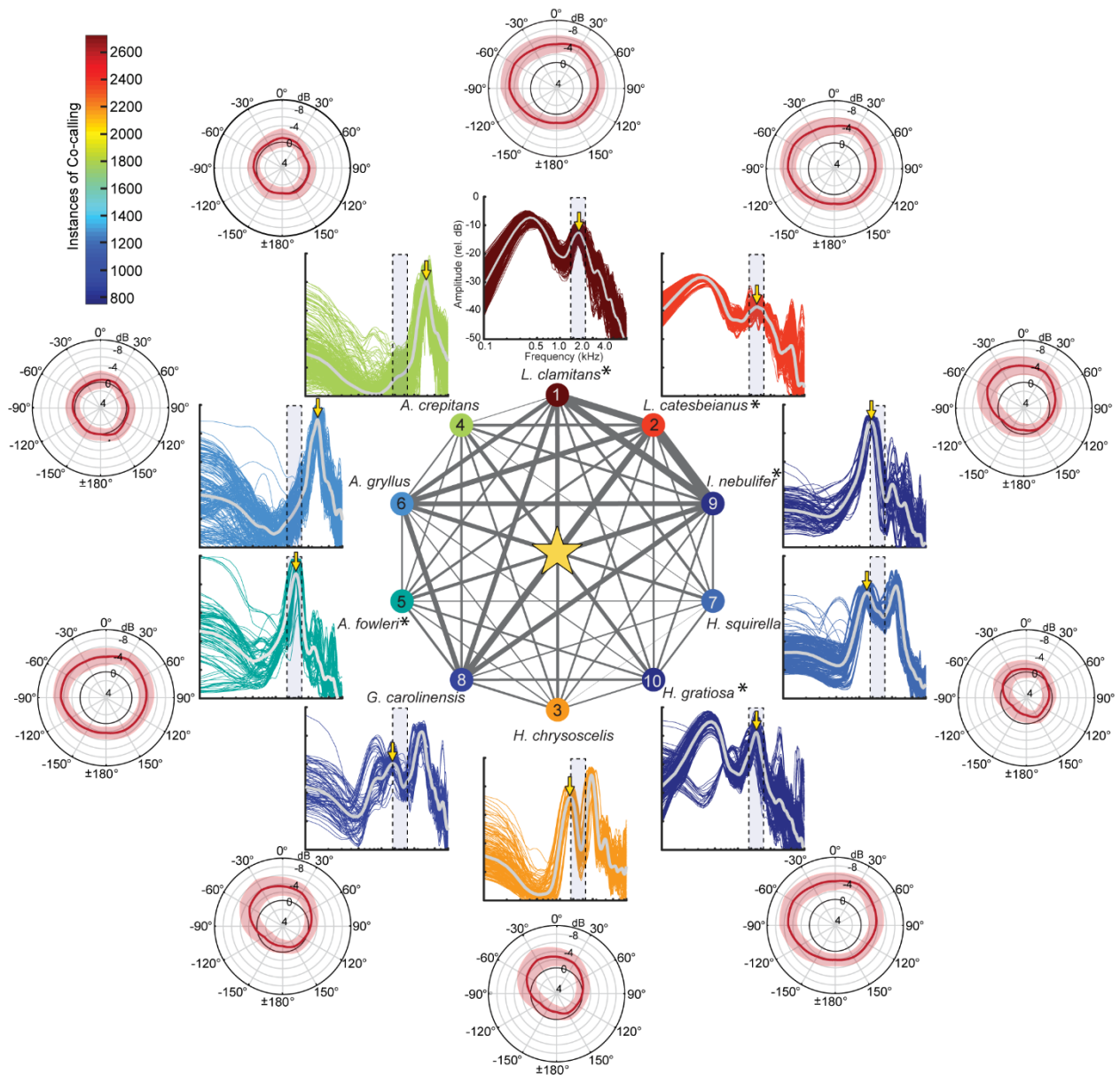
Figure 5
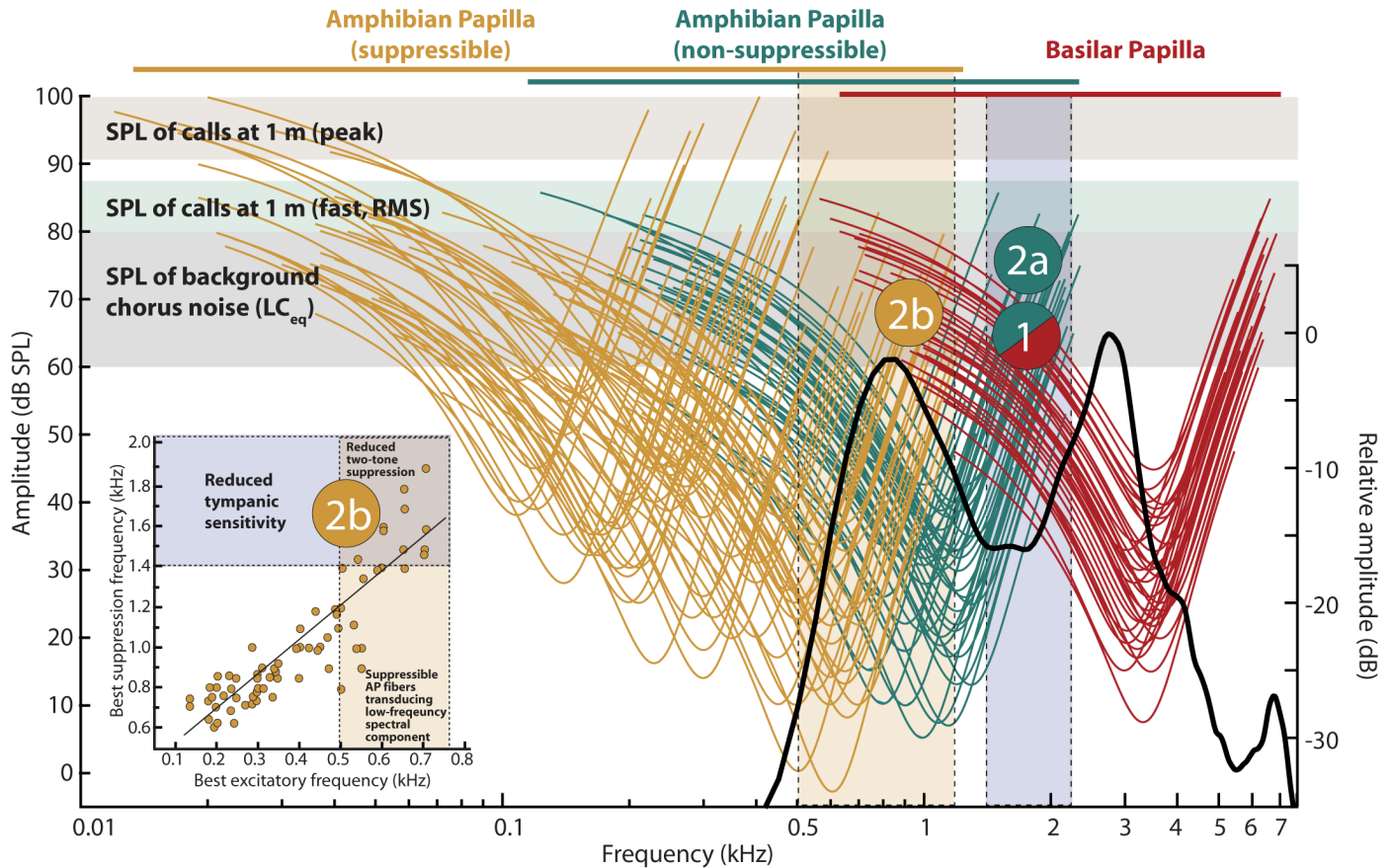
Fig. 5. Lung mediated notch filtering sharpens peripheral frequency tuning and reduces energetic masking and two-tone rate suppression. Modeled tuning curves for 172 auditory nerve fibers in green treefrogs are shown in relation to the frequency range of lung-mediated reductions in tympanum sensitivity (1400 to 2200 Hz, right shaded blue rectangle), the spectrum of conspecific calls (solid black line redrawn from Fig. 3A), and the sound pressure levels (SPLs) of conspecific advertisement calls (*49*) and background chorus noise for a closely-related treefrog (*50*). Tuning curves are depicted separately for low-frequency and mid-frequency fibers innervating the amphibian papilla (AP) and for high-frequency fibers innervating the basilar papilla (BP). Neural responses of low-frequency fibers innervating the AP can be suppressed by frequencies in the range of mid-frequency AP fibers (*36*). The inset shows the best suppression frequency for a given best excitatory frequency for 70 auditory nerve fibers derived from the AP having best excitatory frequencies at or below approximately 700 Hz (redrawn from (*36*)). The greatest two-tone suppression of excitatory responses to a tone presented 10 dB above threshold at a unit's best excitatory frequency was observed when a second tone was simultaneously presented at the unit's best suppression frequency. As the modeled tuning curves illustrate, nerve fibers with best excitatory frequencies in the range of 0.5 to 0.7 kHz transduce the low-frequency spectral component of conspecific calls at the high sound amplitudes used for communication (left shaded gold rectangle). Approximately half of the nerve fibers with best excitatory frequencies within this range can be suppressed by sound energy in the range of 1400 Hz to 1900 Hz. The model predicts two mechanisms by which a reduced tympanum response to frequencies

between 1400 Hz and 2200 Hz is expected to improve sensory processing of conspecific calls. Reduced stimulation by environmental noise of both non-suppressible AP fibers and BP fibers at frequencies where their tuning overlaps ('1') would reduce energetic masking of both spectral components in conspecific calls. Reduced stimulation of non-suppressible AP fibers ('2a') would additionally reduce two-tone rate suppression of high-frequency, suppressible AP fibers ('2b') that transduce the low-frequency component of the call.

Figure 6

Fig. 6. Lung mediated notch filtering improves the signal-to-noise ratio for communication by reducing the tympanum's response to environmental noise. The central figure depicts the social network of co-calling between green treefrogs (star) and the top-10 heterospecific species identified from the NAAMP dataset (Fig. S3). Network edges reflect the relative number of observations of co-calling. Five of the top-10 species produce calls with substantial acoustic energy in the range of reduced tympanum vibration amplitude (asterisks; Table S1). Surrounding the network are depictions of the frequency spectra of each heterospecific species' advertisement calls. Gray lines depict the mean spectrum, averaged over all individuals and calls; colored lines depict the spectrum for each analyzed call and are scaled in color according to the instances of co-calling with green treefrogs (color bar). The shaded blue rectangle in each spectrum represents the frequency range of maximal reduction in the green treefrog's tympanum vibration

amplitude (1400 to 2200 Hz) as a result of lung inflation. Surrounding the spectra are polar plots depicting the mean ± 95% CI difference (in dB) in the tympanum's response between the inflated and deflated conditions (inflated – deflated) at the frequency indicated by a downward pointing yellow arrow on each spectrum ($n = 21$ individuals).

Table S1. Lung-mediated reductions in the tympanum's response to frequencies in heterospecific calls

Species	Sound incidence	Amplitude reduction (dB)	*t*	*p*	df
Lithobates clamitans	0°	4.4 ± 2.0	4.38	< 0.001	20
	-30°	4.6 ± 2.2	3.98	0.001	20
	-60°	5.4 ± 2.2	4.90	< 0.001	20
Lithobates catesbeianus	0°	4.0 ± 1.9	4.06	0.001	20
	-30°	4.2 ± 2.2	3.70	0.001	20
	-60°	5.0 ± 2.1	4.76	< 0.001	20
Incilius nebulifer	0°	4.0 ± 2.0	3.83	0.001	20
	-30°	4.5 ± 2.6	3.43	0.003	20
	-60°	3.8 ± 2.5	3.01	0.007	20
Anaxyrus fowleri	0°	3.6 ± 1.9	3.63	0.002	20
	-30°	3.8 ± 2.2	3.39	0.003	20
	-60°	4.6 ± 2.1	4.43	< 0.001	20
Hyla gratiosa	0°	4.4 ± 2.0	4.38	< 0.001	20
	-30°	4.6 ± 2.2	3.98	0.001	20
	-60°	5.4 ± 2.2	4.90	< 0.001	20

Mean (± 95% CI) reduction in tympanum amplitude vibration as a result of lung inflation in response to the spectral component in or closest to the range of 1400 to 2200 Hz in five heterospecific species' advertisement calls in the frontal field (0°) or in the contralateral field (-30° and -60°) relative to the position of the measurement laser. The species included here represent the five species from among the top-10 co-callers for which the benefit to green treefrogs of lung-mediated reductions in tympanum vibration amplitude would be most pronounced. These co-callers produce advertisement calls with substantial acoustic energy in the frequency range of 1400 to 2200 Hz and frequently co-occur with green treefrogs according to the North American Amphibian Monitoring Program dataset (Fig. 6; Fig. S3). Statistical results are from two-tailed, one-sample t-tests (*n* = 21 individuals).

800

Figure S1
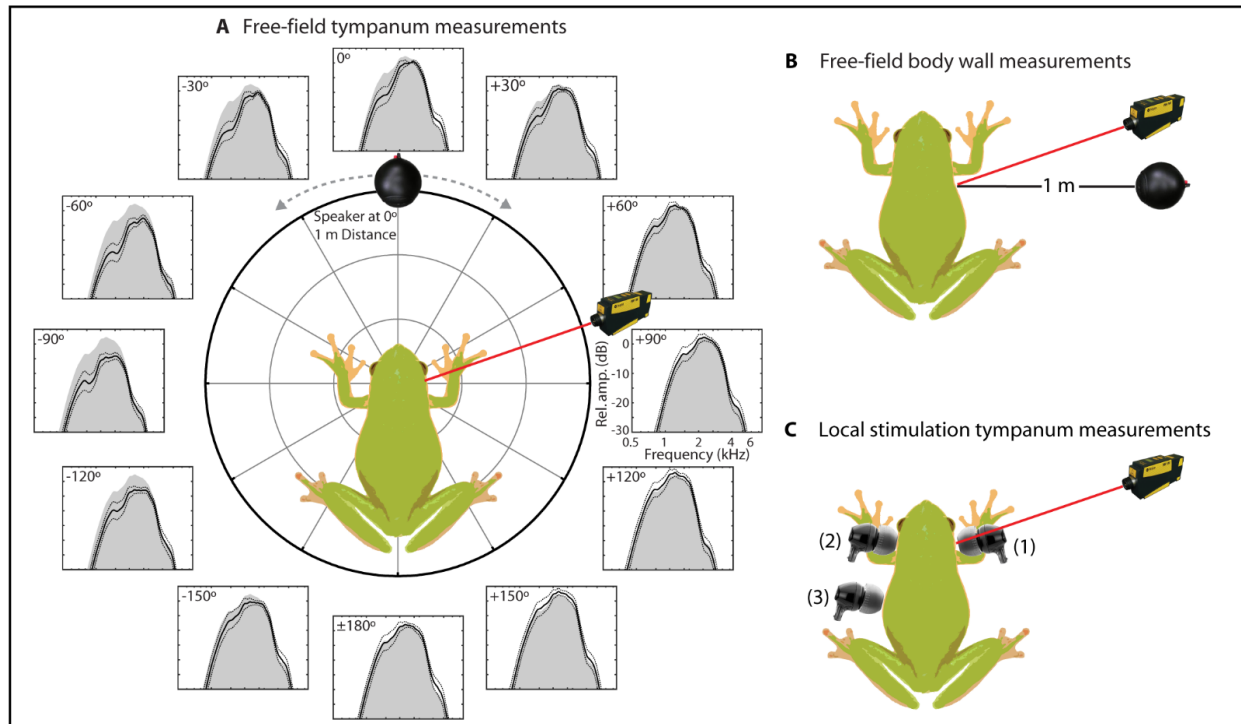
Fig. S1. Laser vibrometry was used to measure the vibration amplitudes of the right tympanum and right body wall overlying the lung in response to acoustic stimulation. (A) The frequency spectrum of the vibration amplitude of the right tympanum was measured under free-field acoustic conditions in response to an FM sweep presented at each of 12 sound incidence angles (0° to ±180° in 30° steps) surrounding the animal from a speaker located 1 m away. These measurements were used to determine the impacts of the lungs on the tympanum's response under conditions of free-field acoustic stimulation. *Insets*: Spectra show the tympanum's mean (solid black line) ± 1 SD (dashed black lines) relative vibration amplitude as a function of frequency and sound incidence angle; the shaded gray area corresponds to the spectrum at +90° and is reproduced for comparison purposes at all other angles of sound incidence. **(B)** The frequency spectrum of the vibration amplitude of the right body wall overlying the lung was measured under free-field acoustic conditions in response to an FM sweep presented from a speaker located 1 m away at an ipsilateral (+90°) angle of sound incidence. These measurements were used to determine the resonance frequency of the lungs under conditions of free-field acoustic stimulation. **(C)** Local acoustic stimulation of the ipsilateral (to the laser) tympanum (1), the contralateral tympanum (2), and the contralateral body wall (3) was used to generate quantitative measures of the transmission gain of indirect sound input to the internal surface of the ipsilateral tympanum via the lungs and the contralateral tympanum. The laser used for measurements was always located at to the frog's right side at an angle of +70° relative to the snout (at 0°).

Figure S2
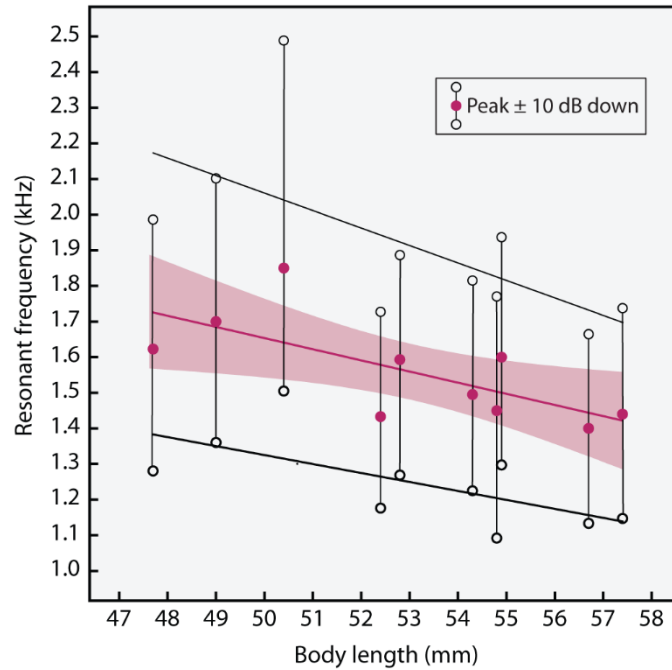
Fig. S2. Frog lungs are size-dependent resonators. Under free-field acoustic stimulation by an FM sweep, the inflated lungs of green treefrogs exhibit a size-dependent resonance. Filled circles depict, as a function of body length, the mean peak resonance frequency of the body wall overlying the right lung in response to free-field acoustic stimulation by an FM sweep and measured using laser vibrometry. Open circles connected to each peak frequency represent the ± 10-dB down points on the resonance spectrum measured relative to the amplitude of the peak frequency. The colored line is the best-fit regression line (±95% CIs) for the peak frequency; black lines depict best-fit lines for the upper or lower 10-dB down points.

Figure S3
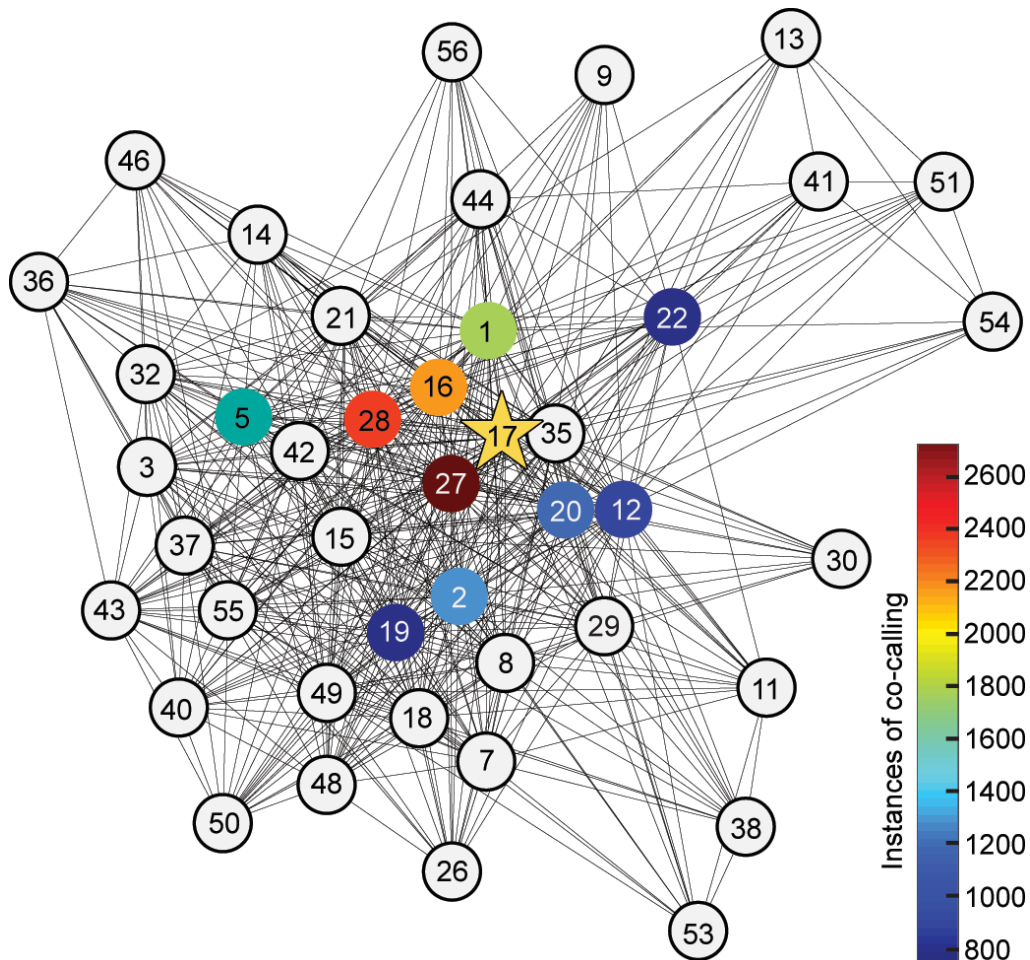
Fig. S3. Social network analysis of data from the North American Amphibian Monitoring Program (NAAMP) identified 42 heterospecific, co-calling species. Using network analysis, we determined the incidence of "co-calling" between green treefrogs and other calling frog species in the NAAMP dataset. Green treefrogs were present on 9245 (2.9%) of the observations in the NAAMP dataset. Within these observations, a total of 42 heterospecific species co-called with green treefrogs. The top-ten co-callers are indicated by colored circles, with the number of observations of co-calling for each species (out of 19,809 total co-calling observations) depicted by the color map. The species identity for each numbered node is as follows: 1 *Acris crepitans*, 2 *Acris gryllus*, 3 *Anaxyrus americanus*, 5 *Anaxyrus fowleri*, 7 *Anaxyrus quercicus*, 8 *Anaxyrus terrestris*, 9 *Eleutherodactylus cystignathoides*, 11 *Eleutherodactylus planirostris*, 12 *Gastrophryne carolinensis*, 13 *Gastrophryne olivacea*, 14 *Hyla andersonii*, 15 *Hyla avivoca*, 16 *Hyla chrysoscelis*, 17 *Hyla cinerea*, 18 *Hyla femoralis*, 19 *Hyla gratiosa*, 20 *Hyla squirella*, 21 *Hyla versicolor*, 22 *Incilius nebulifer*, 26 *Lithobates capito*, 27 *Lithobates catesbeianus*, 28 *Lithobates clamitans*, 29 *Lithobates grylio*, 30 *Lithobates heckscheri*, 32 *Lithobates palustris*, 35 *Lithobates sphenocephalus*, 36 *Lithobates sylvaticus*, 37 *Lithobates virgatipes*, 38 *Osteopilus septentrionalis*, 40 *Pseudacris brimleyi*, 41 *Pseudacris clarkii*, 42 *Pseudacris crucifer*, 43 *Pseudacris feriarum*, 44 *Pseudacris fouquettei*, 46 *Pseudacris kalmi*, 48 *Pseudacris nigrita*, 49 *Pseudacris ocularis*, 50 *Pseudacris ornata*, 51 *Pseudacris streckeri*, 53 *Rhinella marina*, 54 *Scaphiopus couchii*, 55 *Scaphiopus holbrookii*, 56 *Scaphiopus hurterii*, 57 *Spea bombifrons*.